Radio Science, Volume 33, Number 6, Pages 1781–1792, November–December 1998

Ionospheric *D* region remote sensing using VLF radio atmospherics

S. A. Cummer
Laboratory for Extraterrestrial Physics, NASA Goddard Space Flight Center
Greenbelt, Maryland

U. S. Inan and T. F. Bell
Space, Telecommunications and Radioscience Laboratory, Stanford University, Stanford, California

Abstract. Lightning discharges radiate the bulk of their electromagnetic energy in the very low frequency (VLF, 3–30 kHz) and extremely low frequency (ELF, 3–3000 Hz) bands. This energy, contained in impulse-like signals called radio atmospherics or sferics, is guided for long distances by multiple reflections from the ground and lower ionosphere. This suggests that observed sferic waveforms radiated from lightning and received at long distances (>1000 km) from the source stroke contain information about the state of the ionosphere along the propagation path. The focus of this work is on the extraction of nighttime *D* region electron densities (in the altitude range of ~70–95 km) from observed VLF sferics. In order to accurately interpret observed sferic characteristics, we develop a model of sferic propagation which is based on an existing frequency domain subionospheric VLF propagation code. The model shows that the spectral characteristics of VLF sferics depend primarily on the propagation path averaged ionospheric *D* region electron density profile, covering the range of electron densities from $\sim 10^0$ to 10^3 cm^{-3}. To infer the *D* region density from observed VLF sferics, we find the electron density profile that produces a modeled sferic spectrum that most closely matches an observed sferic spectrum. In most nighttime cases the quality of the agreement and the uncertainties involved allow the height of an exponentially varying electron density profile to be inferred with a precision of ~0.2 km.

1. Introduction

Radio atmospherics (or sferics, for short) are the electromagnetic signals launched by individual lightning discharges. Lightning radiates electromagnetic energy over an extremely wide bandwidth, from a few hertz [*Burke and Jones*, 1992] to many tens of megahertz [*Weidman and Krider*, 1986]. However, most of the energy is radiated in the very low frequency (VLF, 3–30 kHz) and extremely low frequency (ELF, 3–3000 Hz) bands. VLF and ELF energy radiated near the ground is reflected by the lower ionosphere and by the ground and thus propagates in a guided fashion between these two boundaries, which form what is known as the Earth-ionosphere waveguide. This guided propagation occurs with low attenuation rates (a few decibels per 1000 km [*Taylor*, 1960]), allowing VLF and ELF sferics to be observed literally around the world from their source lightning discharge. The characteristics of observed sferics are thus determined in large part by the propagation effects introduced by the Earth-ionosphere waveguide, and observed sferics could be used to remotely sense the variable upper boundary, namely the lower ionosphere.

It is generally difficult to measure the ionospheric *D* region (<95 km) electron density, especially at night. Ionosondes and incoherent scatter radars usually do not receive significant echos from this region, where the electron density is typically $< 10^3$ cm^{-3}

Paper number 98RS02381.
0048-6604/98/98RS-02381$11.00

[*Hargreaves*, 1992; *Mathews et al.*, 1982], and the D region is too low in altitude for conventional satellites to make in situ measurements yet too high for balloons. A summary of D region measurement techniques can be found in the work of *Sechrist* [1974]. Most D region measurements to date have been made with rockets, either with Langmuir probes measuring in situ electron density or with HF transmitters, the signals from which are received on the ground and used to infer the electron density of the medium through which the signals propagated [*Mechtly et al.*, 1967].

The fact that VLF waves are almost completely reflected by the D region makes them a useful tool for measuring electron density in this altitude range. Steep and oblique incidence VLF and LF radio wave reflection data have been inverted to derive D region electron density profiles [*Deeks*, 1966; *Thomas and Harrison*, 1970]. Single-frequency VLF propagation measurements have also been used to estimate D region electron density parameters along a given propagation path [*Bickel et al.*, 1970; *Thomson*, 1993].

In this work we develop a new D region measurement technique based on wideband, long-distance VLF propagation effects observed in sferics. In order to accurately interpret observed sferic characteristics, we first develop a model of sferic propagation that is based on an existing frequency domain subionospheric VLF propagation code [*Pappert and Ferguson*, 1986]. To infer the D region density from VLF sferic observations, we find the electron density profile (in a two-parameter family of profiles) that produces a modeled sferic spectrum that most closely matches an observed sferic spectrum. This technique is significantly different from most of those mentioned above in that it is not a point measurement; rather, it is sensitive to the average electron density profile across the entire path, making it uniquely capable of measuring electron density of large regions.

There are significant differences between sferics observed under nighttime and daytime ionospheres [*Chapman and Pierce*, 1957] because the D region ionosphere is a significantly better reflector at night than during the day. Much of the information contained in nighttime sferics is simply not present in daytime sferics, and for this reason we only consider the measurement of nighttime D region profiles from sferic measurements.

Observed sferics have been used in the past to study wideband VLF attenuation and phase velocity [*Jean et al.*, 1960; *Taylor*, 1960]. More recent work with sferics has focused on measurements and theoretical understanding of the long-delayed sferic components which form the "tweek" [*Yamashita*, 1978; *Ryabov*, 1992; *Yedemsky et al.*, 1992], while other research has used measured sferics to determine the distance and geographic bearing to the source discharge and to estimate the ionospheric reflection altitude along the propagation path [*Kumar et al.*, 1994; *Hayakawa et al.*, 1994]. *Rafalsky et al.* [1995] employed a technique similar to that used in this work to infer the effective ionospheric reflection height from sferic observations, but the precision of the method was somewhat limited by the fact that the precise source locations were not known.

2. Sferic Observations

The sferics presented in this work were recorded with the Stanford University VLF radiometer [*Fraser-Smith and Helliwell*, 1985] with a triangular loop receiving antenna oriented ~95° east of geographic north. The receiver is located at 37.43°N, 122.16°W. The digitized magnetic field has a 3 dB bandwidth from 420 Hz to 20 kHz. There is an uncertainty of ~5% in the absolute amplitude calibration for the data; however, this uncertainty does not affect the ionospheric measurements made in this work, which do not depend on the absolute field amplitude.

2.1. Individual Sferics

Figure 1a shows a typical sferic waveform received at Stanford from a relatively large (−56 kA peak current) cloud-to-ground (CG) lightning discharge that occurred in the midwestern United States. The semidiscrete pulses in the tail of the waveform can be interpreted as signals which propagated along individual ray paths with a different number of reflections from the ground and ionosphere [*Chapman and Pierce*, 1957]. Figure 1b shows a spectrogram (produced using a method described by *Kim and Ling* [1993] designed for signals of this type) of this waveform. The time-frequency representation of the sferic shows it to be a superposition of dispersed elements whose group velocity is slow near their particular cutoff frequencies. Each of these elements represents an individual mode in the Earth-ionosphere waveguide. Figure 1c shows the amplitude of the sferic in the frequency domain, computed using the fast Fourier

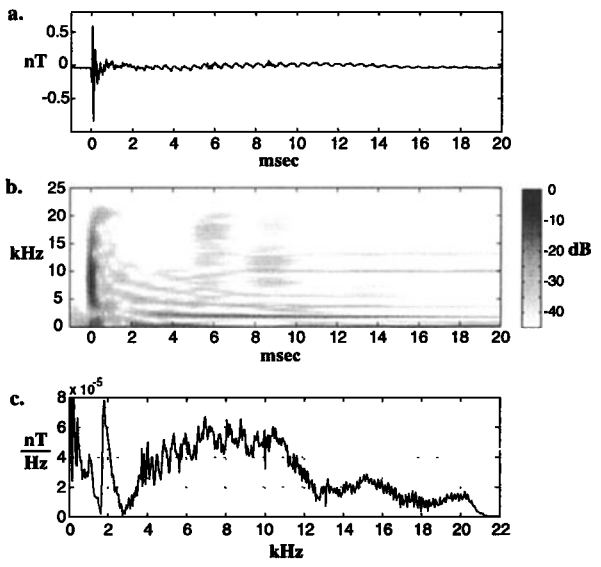

Figure 1. (a) waveform, (b) spectrogram, and (c) spectrum of a representative large sferic.

transform (FFT). The amplitude variations with frequency are created by the constructive and destructive interference of waveguide modes with phase velocities which vary with frequency at different rates. At lower frequencies (from ~3 to 8 kHz) the amplitude variations are fairly simple because of the small number of modes. At higher frequencies, more modes are involved, and the interference produces more complicated variations.

All of these sferic representations contain the same information about the ionosphere since they were created by the propagation of the signal in the Earth-ionosphere waveguide. However, the information we are after is most readily quantified in the spectral amplitude, and it is from this quantity that the ionospheric measurement will be extracted.

2.2. Sferic Averaging

The noise level in the spectrum of a single observed sferic is low enough that the fine structure is visible, but an improvement in the signal-to-noise ratio should provide a more accurate D region electron density measurement. This can be accomplished with standard superposed epoch analysis, in which a number of individual sferics are accurately time aligned and averaged to decrease the noise and isolate the signal of interest. However, care must be taken to average only sferics that are known to have originated from a small geographic location so that the propagation effects on their spectrum are identical. The National Lightning Detection Network (NLDN) provides the location and time of an individual discharge to an accuracy of a few kilometers and better than 1 ms [*Bernstein et al.*, 1996], which allows the unique identification of the source location of an individual sferic (which also must be known to accurately model the sferic propagation). To produce an average sferic spectrum, we average the sferics determined by the NLDN to have originated in a 0.5° latitude by 0.5° longitude region (~56 km by 48 km at latitudes of the continental United States). The sferics are taken from a 30 min period, which is long enough to include enough sferics for effective averaging but is short enough that the large-scale D region density is not likely to change significantly. For the periods considered in this work the distribution of sferic amplitudes included in the averaging spans approximately a factor of 4, with the majority of sferics having a peak amplitude near the center of this distribution, so that the average spectra computed are not dominated by a small number of sferics.

The noise level can also be improved by taking advantage of the fact that after the first few milliseconds of the sferic, only frequency components below ~10 kHz remain (this is because the long-delayed, near-cutoff components become strongly attenuated with increasing frequency). Thus, before averaging, the individual sferic waveforms are low-pass-filtered below 10 kHz after 4 ms from their onset, thereby significantly reducing the noise level above 10 kHz.

As an example of the overall averaging and filtering procedure, we show observations from July 22, 1996, between 0415 and 0445 UT. There were 59 sferics launched from the region 37.3°–37.8°N and 99.4°–99.9°W that met the criteria to be included in the averaging. The first 18 ms of each sferic were included in the temporal averaging. Figure 2 shows the average sferic spectral amplitude on two different scales to highlight the details of the signal. A comparison of this spectrum with that of the individual sferic in Figure 1 clearly shows that the averaging significantly improves the signal-to-noise ratio and reinforces the fine spectral features that we will use as the basis of the D region measurement.

3. Modeling Sferic Propagation

Our D region measurement technique compares an averaged observed sferic spectrum against a model

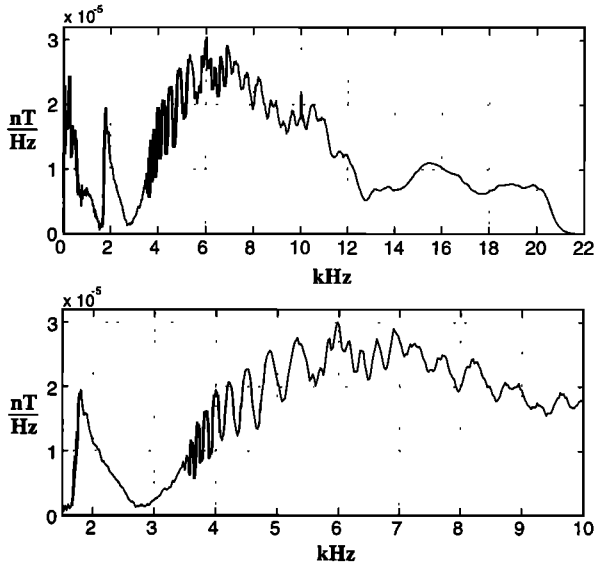

Figure 2. Average sferic spectrum calculated from 59 individual sferics, shown on two frequency scales to emphasize the fine structure. The fine structure is much cleaner compared to the single-sferic spectrum in Figure 1.

calculation to infer the ionospheric D region electron density profile. There are analytical VLF propagation models which can produce sferic spectra [e.g., *Sukhorukov*, 1996], but for our purposes the sferic propagation model must accurately account for all of the factors that significantly affect the propagation, such as the arbitrary orientation of the ambient magnetic field, the nonperfectly conducting ground, and the effect of ions on the ionospheric medium. The basis for our sferic model is a single-frequency VLF-ELF propagation model, called LWPC, which was developed by the U.S. Navy [*Pappert and Ferguson*, 1986] and which includes all of these effects. This model solves the time-harmonic (i.e., single frequency) propagation problem using mode theory [*Budden*, 1961], in which the fields at a distance from the source are described as a sum of independently propagating waveguide modes.

The transverse horizontal magnetic field B_y at a distance x along the ground from a vertical electric dipole source as a function of frequency is

$$B_y(\omega,x) = -\mu_0 k^{\frac{1}{2}} M_e(\omega) \left[R_e \sin\left(\frac{x}{R_e}\right)\right]^{-\frac{1}{2}} \cdot \left(\frac{\pi}{2}\right)^{-\frac{1}{2}} e^{\imath\frac{\pi}{4}} \sum_n \Lambda_{tn}\,\Lambda_{rn}\, e^{-\imath k x \sin\theta_n}. \quad (1)$$

The wavenumber $k = 2\pi/\omega$, $M_e(\omega)$ is the vertical electric dipole moment of the source (and is related to the source current by $M_e(\omega) = -iIl/\omega$, where I is the source current amplitude and l is the length of the current channel), and the term $[R_e \sin(x/R_e)]^{-1/2}$ accounts for the spreading of the fields over a spherical Earth of radius R_e (note that this term is equivalent to $x^{-1/2}$ over short distances). The summation is over the significant modes (evanescent and strongly attenuated modes are excluded), each of which has an index of refraction given by the sine of the corresponding eigenangle θ_n, and also excitation and receiver factors Λ_{tn} and Λ_{rn}, in which the altitude dependence of the fields is contained. The reader is referred to *Pappert and Ferguson* [1986, and references therein] for further details concerning this model.

To calculate the fields from a broadband source, one simply needs to calculate $B_y(\omega)$ over the range of frequencies significant to the problem at hand (in our case, from 1.5–22 kHz). The resulting sferic spectrum can be converted to a time-domain waveform with an inverse Fourier transform operation, but this is not necessary for our purposes, as we evaluate the sferic spectra rather than the waveforms.

Most of the propagation effects are contained in the Λ_{tn}, Λ_{rn}, and $\sin\theta_n$ terms in (1). Many different parameters of the Earth-ionosphere waveguide have a significant effect on these quantities, each of which is addressed individually in sections 3.1–3.5.

3.1. Ionospheric Electron Density

For the purposes of low-power VLF propagation the ionosphere can be fully characterized by its electron and ion density profiles, the corresponding collision frequency profiles, and the direction and intensity of any ambient magnetic field. However, the altitude range of the ionosphere that plays a role in the guiding of VLF and ELF waves depends on the particular frequency of interest and limits the region that can be probed with this VLF-based technique. It is known that ELF propagation is affected by electron densities from D to F region altitudes (~60–300 km) [*Pappert and Moler*, 1974; *Barr*, 1977]. However, modeling indicates that for the assumed electron-neutral collision frequency profile of (3) in section 3.3, VLF propagation from 3 to 22 kHz is primarily affected only by electron densities between 10^0 and 10^3 cm^{-3}, and we conclude that this is the range of electron densities that is measurable using the sferic-based technique in this work.

The electron density profile in the D region, the quantity we aim to measure, is known to be highly variable [*Budden*, 1985, p. 12]. We calculate the model sferic spectrum under a number of different ionospheres to find that which most closely matches the measured sferic spectrum. This procedure requires a parameterization of the electron density profile so that it can be varied in a controlled manner. Throughout this paper, we assume that the D region electron density can be described by a two-parameter exponential profile,

$$N_e(h) = 1.43 \times 10^7 \exp(-0.15h') \cdot \exp[(\beta - 0.15)(h - h')] \text{ cm}^{-3}, \quad (2)$$

with h' in kilometers and β in km^{-1}. The two parameters h' and β control the altitude of the profile and the sharpness of the ionospheric transition, respectively. A larger β implies a more rapid change of N_e with altitude. This specific functional form has been used with success in previous comparisons between VLF propagation theory and measurement [e.g., *Bickel et al.*, 1970; *Thomson*, 1993], and it agrees well with directly observed D region profiles [e.g., *Sechrist*, 1974].

3.2. Ionospheric Ion Density

The effect of free ions on electromagnetic wave propagation in the ionospheric cold plasma can be neglected under many circumstances. However, at the lower end of the VLF spectrum, the wave frequency is close enough to the ion plasma frequency and gyrofrequency to have a potentially significant effect on wave propagation. Sferic model calculations indicate that both positive and negative ions are significant (though not dominant), especially for propagation below 10 kHz, and their effects will be included in all of the calculations herein. Although many different ion species are present at D region altitudes, the LWPC propagation model lumps their effect into a single species with atomic mass 32, which is a reasonable approximation to the known dominant species [*Narcisi and Bailey*, 1965]. As a rough approximation to the daytime observations of *Narcisi* [1971], we assume that the positive ion density is constant below the altitude where N_e equals some predetermined value $N_i^{+\min}$, so that $N_i^+ = N_i^{+\min}$. Above this altitude, $N_i^+ = N_e$. To maintain charge neutrality, N_i^- is defined by $N_i^- = N_i^+ - N_e$. *Narcisi* [1969] reported rocket-based midlatitude nighttime ion measurements in the presence of a sporadic E layer at ~90 km, which showed a total positive ion density $< 3\times10^2$ cm^{-3} below 80 km. We assume that $N_i^{+\min} = 3\times10^2$ cm^{-3}, except in section 6.1 in which we investigate the errors introduced by this assumption. Simulations show that this is a level at which the effect of ions is significant but not dominant.

3.3. Electron and Ion Collision Frequency

The ionospheric electron-neutral collision frequency used in this work is an analytical approximation of experimental data and is given by [*Wait and Spies*, 1964]

$$\nu_e = 1.816\times10^{11} \exp(-0.15z) \text{ s}^{-1}, \quad (3)$$

where z is the altitude measured in kilometers. The ion-neutral collision frequency is given by [*Morfitt and Shellman*, 1976]

$$\nu_i = 4.54\times10^9 \exp(-0.15z) \text{ s}^{-1} \quad (4)$$

for both positive and negative ions. The ion and electron collision frequency profiles are known to be less variable than the ion and electron density profiles [*Budden*, 1985, p. 12], and modeling has shown that changing the collision frequencies by a factor of 2 has only a small effect on sferic propagation. For these reasons the electron and ion collision frequency profiles are assumed to be fixed.

3.4. Ground and Magnetic Field Parameters

The ground forms the lower boundary of the Earth-ionosphere waveguide, while the Earth's magnetic field has a strong effect on the electromagnetic parameters of the ionospheric plasma. The ground conductivity, ground permittivity, and ambient magnetic field are treated as homogeneous along the waveguide, and they are determined in the LWPC model from built-in geographic maps of these quantities. For all of the overland propagation paths considered in this work, the relative permittivity of the ground is taken to be 15, and the ground conductivity is between 0.01 and 0.03 mho·m^{-1}. Model calculations show that this measurement technique is insensitive to the precise value of the assumed ground conductivity provided it is greater than $\sim 3 \times 10^{-4}$ mho·m^{-1}. While, in general, lowering conductivity does increase VLF attenuation, this effect is somewhat frequency independent, and it is only for conductivities below this value that the relative modal

attenuation rates change enough to disturb the measurement. The magnetic field parameters depend slightly on the precise path location but are given approximately by an amplitude of $\sim 5.2 \times 10^4$ nT, a dip angle of $\sim 55°$, and an azimuthal angle relative to the propagation direction of $\sim 250°$ counterclockwise.

3.5. Lightning Return Stroke

Sferics are radiated by the vertical current-moment (current × channel length) in the lightning return stroke [*Arnold and Pierce*, 1964]. Lightning return stroke spectra are usually smooth through the VLF band [*Lanzerotti et al.*, 1989], so in a sferic spectrum the broad-scale source effects should be separable from the fine-scale propagation effects. We will compare the observed and modeled spectra by focusing only on the details of the spectrum, making the measurement technique independent of the large-scale spectral variations (and therefore independent of the source spectrum). However, for the complete modeled and observed sferic spectra to agree well, we include a particular functional form for the lightning current moment waveform in the modeled sferic spectra plotted throughout this work. The model return stroke has a current moment of [*Jones*, 1970]

$$I_m(t) = i_{g0}\frac{v_0}{\gamma}\left[e^{-at} - e^{-bt}\right]\left[1 - e^{-\gamma t}\right] \quad \text{A} \cdot \text{m}. \quad (5)$$

Dennis and Pierce [1964] concluded from a review of data that reasonable parameter values are $i_{g0} = 20$ kA, $a = 2 \times 10^4$ s^{-1}, $b = 2 \times 10^5$ s^{-1}, $v_0 = 8 \times 10^7$ m·s^{-1}, and $\gamma = 3 \times 10^4$ s^{-1}, and the values used to produce the spectra shown in this work are close to these.

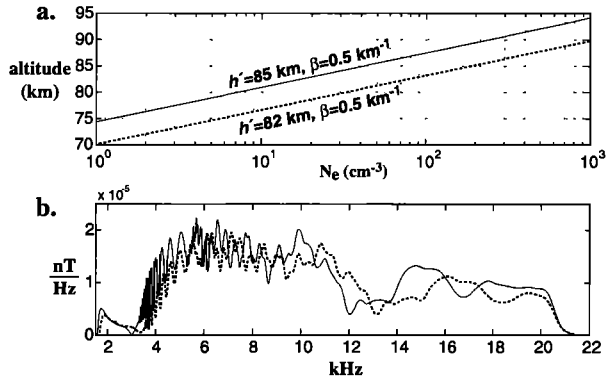

Figure 3. A comparison of sferic spectra for two nighttime ionospheres with different values for h', (a) two nighttime D region density profiles and (b) sferic spectra for the profiles in Figure 3a.

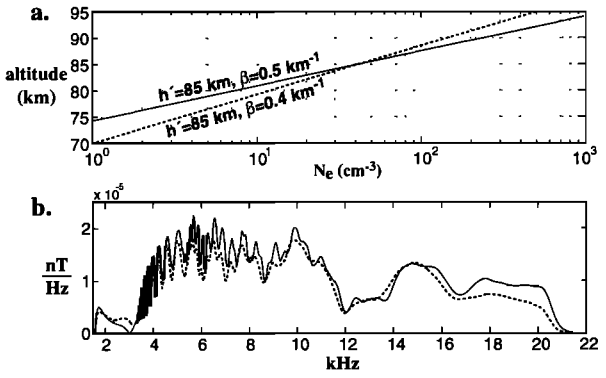

Figure 4. A comparison of sferic spectra for two nighttime ionospheres with different values for β, (a) two nighttime D region density profiles and (b) sferic spectra for the profiles in Figure 4a.

4. Effect of Electron Density on the Sferic Spectrum

Before extracting electron density profiles from sferics, it will be helpful to understand the effect of the electron density profile parameters h' and β on the characteristics of sferics. We investigate these effects on a propagation path of length 1960 km from 37°N, 100°W to Stanford.

4.1. Ionospheric Height h'

Figure 3a shows two nighttime electron density profiles with different heights ($\beta = 0.5$ km^{-1} and $h' = 85$ and 82 km), and Figure 3b shows the theoretical sferic spectra calculated for each of these profiles. The difference between the two spectra is quite clear: the spectrum corresponding to the higher reflection height is compressed relative to that with the lower reflection height, but it maintains the same general shape. This effect is not surprising, as a higher waveguide boundary lowers the cutoff frequencies of individual modes in the waveguide, causing the compression of the spectrum.

4.2. Ionospheric Sharpness β

The effect of β on sferic characteristics is more subtle. Figure 4a shows two nighttime electron density profiles with different sharpness parameters ($h' = 85$ km and $\beta = 0.5$ and 0.4 km^{-1}), and Figure 4b shows the sferic spectra for each. The spectrum for the

$\beta = 0.4$ profile is significantly smoother than that for $\beta = 0.5$, especially above 10 kHz, and the amplitude of the modal interference variations at lower frequencies is slightly smaller for the smaller β. Qualitatively, these effects are expected, since the sharper ionosphere is a better reflector and this improved reflection correspondingly decreases the attenuation of the most vertically propagating modes, namely those near cutoff. This decreased attenuation accounts for the increased amplitude of these modes, in turn enhancing the modal interference variations. The above analysis shows that the effects of h' and β are significant in both the sferic waveforms and sferic spectra for a nighttime ionosphere, and thus they should be distinguishable in observed sferics.

5. Ionospheric Measurement Examples

We are now ready to extract the ionospheric parameters h' and β by comparing the fine features of an observed sferic spectrum with those from a number of modeled spectra to find the parameters which produce the best agreement. However, we need to construct a way of quantifying the agreement between the fine features of the observed and modeled sferic spectra. An effective way to extract these fine features is to normalize the spectrum by a smoothed version of the same spectrum to produce a new function containing only the smaller variations of the original. Figure 5 shows an example of this detail extraction.

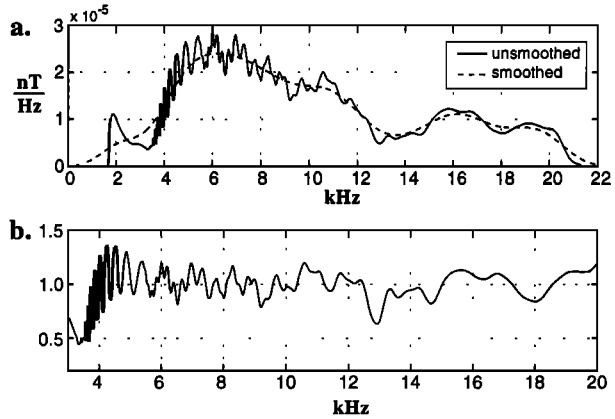

Figure 5. Demonstration of spectral detail extraction showing (a) modeled unsmoothed and smoothed sferic spectra and (b) the spectral detail function extracted from the sferic spectrum.

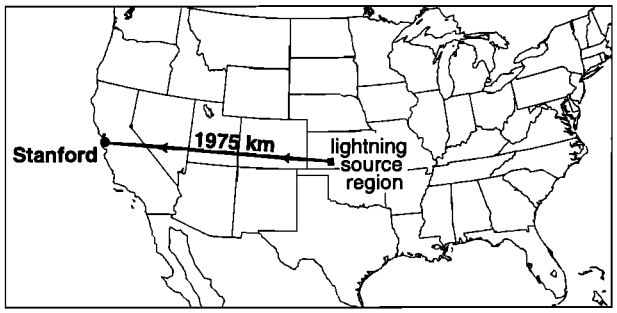

Figure 6. Map showing the sferic receiver location (Stanford) and the lightning source region on July 22, 1996, 0415-0445 UT.

Once this detail function D is calculated for each of the two spectra to be compared, the agreement between the two functions is quantified by $F = \sum(D_{\text{observed}} - D_{\text{modeled}})^2$, summed over frequencies from 4 to 20 kHz. A smaller F indicates better agreement between theory and observation, and the location of the minimum in β-h' gives the extracted ionospheric parameters. Frequencies below 4 kHz are excluded because they consistently show variations that are not predicted by the propagation model. These variations are possibly due to interference with the quasi-transverse electromagnetic mode (QTEM) of the Earth-ionosphere waveguide, which is usually strongly attenuated at frequencies >1 kHz [*Barr*, 1977]. The propagation of the QTEM mode is influenced by the E and F regions of the ionosphere; thus its presence interferes with the proposed D region measurement.

5.1. Measurement Over a Single Path

We first present a D region measurement made from sferics propagating over a single path. The sferics used here are from a storm on July 22, 1996, between 0415 and 0445 UT. As shown in Figure 6, the source strokes from latitudes 37.3°–37.8°N and longitudes 99.4°–99.9°W launched sferics that were received at Stanford, 1975 km away from the center of this source region.

The average measured sferic spectrum for this case was shown in Figure 2. Figure 7a shows a contour plot of F versus β and h' for this path and time period. The best agreement is at the location of the minimum of F in β-h' space; thus $h' = 83.3$ km and $\beta = 0.49$ km^{-1} form the ionospheric measurement.

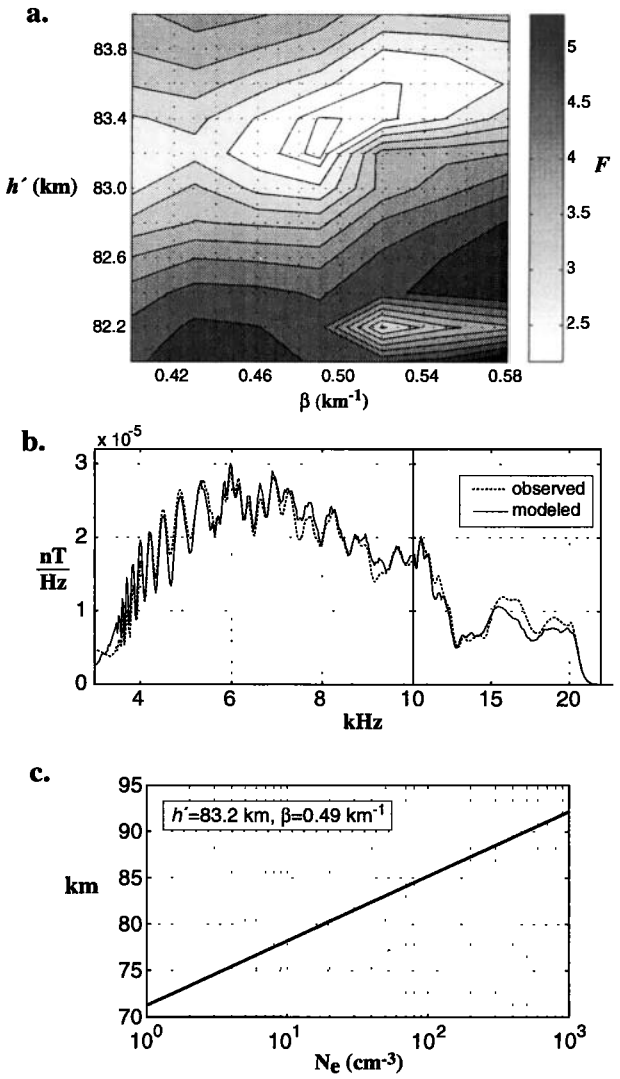

Figure 7. Extraction of ionospheric parameters from measured spectral details. (a) Contour plot of F versus β and h'. The minimum gives the best fit ionosphere for this particular observation. (b) The observed and best fit modeled sferic spectra on a frequency scale highlighting the fine-feature agreement. (c) The measured D region electron density profile.

The plot shows that a change in h' of 0.2 km or in β of 0.01 km^{-1} produces distinguishably worse agreement, indicating the precision of this measurement. Figure 7b shows good agreement between the observed and best fit modeled spectral amplitudes on a frequency scale highlighting the fine-feature agreement. Figure 7c shows the electron density profile defined by these two parameters for $N_e = 10^0$–10^3 cm^{-3} (which is the range of N_e to which the VLF propagation is sensitive, as was discussed in section 3.1).

The modeled spectrum in Figure 7b was calculated using a model return stroke with parameters $a = 10^4$ s^{-1}, $b = 3 \times 10^5$ s^{-1}, and $i_{g0} = 34$ kA, in the notation of (5). These parameters were chosen to give good visual agreement between the broad spectral amplitude of the modeled and observed spectra to highlight the overall agreement between the modeled and observed spectra. By varying the return stroke parameters to achieve good agreement with an observed spectrum, the return stroke waveform could also be inferred from average or individual sferics, but this is not the focus of this work.

An implicit assumption of the LWPC propagation model is that the ground altitude along a propagation path is constant. In reality, this is not a valid assumption for the typical land paths considered here. The electromagnetic boundary conditions at the lower waveguide interface are enforced at the ground altitude, so the propagation is sensitive to the difference of the ionospheric height and the ground height. Thus the inferred path-averaged ionosphere is measured relative to the average ground altitude of the sferic propagation path. This fact must be accounted for when comparing inferred ionospheres along propagation paths with different mean ground altitudes. The mean ground altitude (referenced to sea level) of this propagation path is 1.7 km, implying that $h' = 85.0$ referenced to sea level.

5.2. Simultaneous, Multiple-Location Ionospheric Measurements

Using the same time period as in the previous example (July 22, 1996, 0415–0445 UT), we can also infer D region electron densities along a number of different sferic propagation paths, both to verify the consistency of the ionospheric parameter extraction along paths that overlap and to produce simultaneous D region measurements over a large portion of the continental United States. The three locations (in addition to that of the previous example) that had enough lightning to produce a satisfactory measurement are as follows: 28.1°–28.5°N, 108.9°–109.2°W; 35.2°–35.4°N, 104.5°–104.8°W; and 35.8°–36.2°N, 87.5°–88°W. The mean ground altitudes of these three paths are 0.5 km, 1.6 km, and 1.2 km, respectively.

Figure 8 shows, for each location, the measured average spectrum and the best fit modeled spectrum that produced the ionospheric measurement. Reasonable return stroke parameters are used in (5) to produce the modeled spectra for these four locations. The agreement in the alignment of the fine features between theory and measurement is comparable to the agreement displayed for the previous example in Figure 7. The fact that the fine features between 4 and 20 kHz agree well with the model indicates that the inferred electron density profiles are accurate.

Figure 9 shows a map of the propagation paths to Stanford from these three locations and the one analyzed in section 5.1. Each path is labeled with the inferred ionospheric parameters (h' and β) for this period based on the spectral fits shown in Figure 8. Each h' is referenced to sea level so that the ionosphere over each path can be directly compared. The slight difference in β on the overlapping paths is comparable to the uncertainty of this measurement technique (as discussed in section 6), but if the difference is real it is likely due to the fact that the eastern portion of the longer path was farther removed from sunset and had relaxed more than the western portion. There is also a significant ionospheric height change of ~1 km from the center of the United States to the southernmost portion. It is difficult to place this measurement in the context of other measurements because no simultaneous D region measurement over such a large geographic area has been made before.

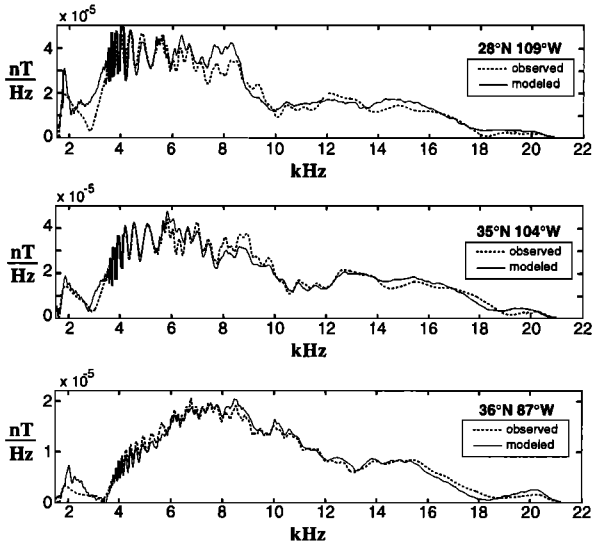

Figure 8. Observed and best fit theoretical sferic spectra on July 22, 1996, from 0415–0445 UT for sferics originating in three other geographic areas.

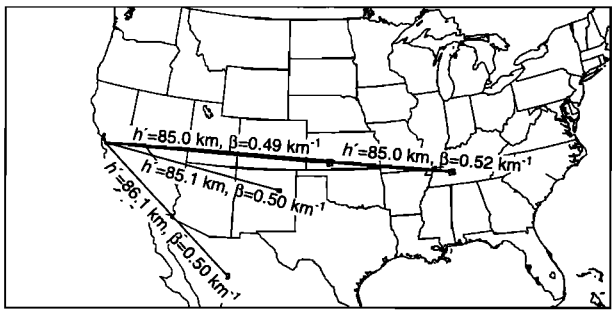

Figure 9. Map of propagation paths to Stanford labeled with simultaneous extracted ionospheric parameters h' (referenced to sea level) and β.

This example highlights the potential of this technique for the measurement of the D region. With just a few more strategically placed receiving stations, these five source regions could produce path-averaged measurements along 20 or more propagation paths. An image of the ionosphere over the entire United States can in principle be produced by a tomographic reconstruction of the spatial variation of D region height and sharpness based on many path-integrated measurements.

6. Uncertainties in the Electron Density Measurement

There are two primary sources of uncertainty in the propagation model which can potentially affect our ionospheric measurement: the unknown ion density profile and the possible presence of ionospheric inhomogeneities. We show that their effects are small, and we estimate the total uncertainty (from modeling uncertainties and the precision of the extraction technique) in h' to be ± 0.3 km and the total uncertainty in β to be ± 0.02 km^{-1}.

6.1. Ion Density

It was mentioned in section 3.2 that variations in our choice of $N_i^{+\min}$ have a demonstrable effect on a modeled sferic spectrum, which suggests that the uncertainty in this quantity could lead to uncertainty in the extraction of h' and β from observed sferics. This uncertainty can be quantitatively investigated by calculating a sferic spectrum with an ion density profile different from the assumed $N_i^{+\min} = 3 \times 10^2$ cm^{-3}

and then by extracting h' and β from this modeled spectrum, assuming the standard ion density profile.

Assuming $h' = 85.0$ km and $\beta = 0.5$ km^{-1}, an ion density of $N_i^{+\min} = 1.5 \times 10^2$ cm^{-3} leads to an extracted ionosphere of $h' = 85.1$ km and $\beta = 0.51$ km^{-1}, while an ion density of $N_i^{+\min} = 6.0 \times 10^2$ cm^{-3} leads to an extracted ionosphere of $h' = 84.8$ km and $\beta = 0.49$ km^{-1}. Clearly, decreasing the ion density raises and sharpens the ionosphere, while increasing the ion density has the opposite effect. However, the magnitude of the effect of a factor of 2 change in the ion density is small in terms of h' and β compared to the observed variations, and it does not significantly affect our ability to accurately infer the D region electron density profile.

6.2. Ionospheric Inhomogeneities

For all of the measurements presented in this paper the ionosphere has been assumed to be homogeneous along the propagation path. In reality, the ionosphere is almost certainly inhomogeneous to some degree, which may introduce further uncertainty in the extracted h' and β. It is important to verify that even in the presence of ionospheric inhomogeneities, sferic characteristics are determined by the path-averaged ionosphere.

To do this, we follow a procedure similar to that in the previous section and calculate a sferic spectrum for a sharply inhomogeneous ionosphere with $h' = 84.0$ km over the propagation path from source to midpoint and $h' = 81.0$ km over the path from midpoint to receiver. The sharpness $\beta = 0.5$ km^{-1} over both portions. Extracting h' and β from this spectrum (assuming a homogeneous ionosphere) yields $h' = 82.5$ km and $\beta = 0.51$ km^{-1}. This shows that the sferic spectrum is controlled by the path-averaged ionospheric height and that the presence of a significant ionospheric height inhomogeneity does not introduce a significant uncertainty in the extracted parameters.

A similar calculation with a constant height ($h' = 82.5$ km) and an inhomogeneous sharpness ($\beta = 0.55$ km^{-1} over the first half of the path, and $\beta = 0.45$ km^{-1} over the latter portion) gives extracted homogeneous ionospheric parameters of $h' = 82.5$ km and $\beta = 0.49$ km^{-1}. This verifies that the sferic spectrum is controlled by the path-averaged ionospheric height and sharpness, even in the presence of significant inhomogeneities in these quantities.

7. Conclusions

We have compared measurements of the characteristics of VLF radio atmospherics with theoretical propagation predictions to infer the nighttime D region electron density profile along the sferic propagation path in the Earth-ionosphere waveguide. A general theoretical formulation for the propagation of single-frequency VLF signals in the Earth-ionosphere waveguide developed by *Budden* [1962] and implemented in a computer code [*Pappert and Ferguson*, 1986, and references therein] was adapted to solve the problem of the propagation of transient VLF signals.

In an effort to understand the range of D region ionospheric parameters that can be inferred using observed VLF sferics, the effects of various ionospheric conditions and parameters on the characteristics of VLF (>1.5 kHz) sferics were theoretically investigated. Because the sferic spectrum was found to be a better indicator of these parameters than the sferic waveform, all comparisons of theory and observation were made in the frequency domain. The details of the sferic spectrum were shown to be strongly dependent on the height and sharpness of a two-parameter model ionosphere.

Observed sferics originating in lightning discharges occurring in a small geographic region (as documented by the National Lightning Detection Network) were temporally averaged to reinforce the propagation effects to be measured and reduce the effects of source variability and noise. Spectra were computed for a number of different ionospheres, and the ionosphere that produced the best agreement with the observed sferic spectrum was extracted. It should be emphasized that this technique infers electron density profiles relative to the average ground altitude of a particular propagation path.

The D region measurement technique was also applied to multiple propagation paths. Simultaneous nighttime measurements using sferics from five different lightning locations (all received at Stanford) showed an ionospheric height increase of 2 km from north to south across much of the United States.

An evaluation of the errors in the measurement introduced by the precision of the extraction, the uncertainty in the ion density profile, and the uncertainty in the ionospheric homogeneity showed that uncertainties of only ± 0.3 km in h' and ± 0.02 km^{-1} in β are to be expected. The observed variation of h' was significantly greater than this uncertainty.

Quantitative evaluation of the accuracy of this measurement technique will have to wait for the development of an independent technique for measuring large-scale *D* region electron densities.

Acknowledgments. This work was supported by the ONR under grants N00014-94-1-0100 and N00014-95-1-1095. S. A. Cummer was supported for a portion of the writing of this paper by a National Research Council Postdoctoral Research Associateship. We thank A. Fraser-Smith of Stanford University for the use of the VLF radiometer, B. Trabucco and J. Yarbrough of Stanford University for help with data handling and acquisition, and F. Perry Snyder of NCCOSC/NRaD for helpful discussions regarding the VLF propagation model.

References

Arnold, H. R., and E. T. Pierce, Leader and junction processes in the lightning discharge as a source of VLF atmospherics, *Radio Sci., 68D*, 771, 1964.

Barr, R., The effect of sporadic-*E* on the nocturnal propagation of ELF waves, *J. Atmos. Terr. Phys., 39*, 1379, 1977.

Bernstein, R., R. Samm, K. Cummins, R. Pyle, and J. Tuel, Lightning detection network averts damage and speeds restoration, *IEEE Comput. Appl. Power, 9*, 12, 1996.

Bickel, J. E., J. A. Ferguson, and G. V. Stanley, Experimental observation of magnetic field effects on VLF propagation at night, *Radio Sci., 5*, 19, 1970.

Budden, K. G., *The Wave-Guide Mode Theory of Wave Propagation*, Logos Press, London, 1961.

Budden, K. G., The influence of the Earth's magnetic field on radio propagation by wave-guide modes, *Proc. R. Soc. London, Ser. A, 265*, 538, 1962.

Budden, K. G., *The Propagation of Radio Waves*, Cambridge Univ. Press, New York, 1985.

Burke, C. P., and D. L. Jones, An experimental investigation of ELF attenuation rates in the Earth-ionosphere duct, *J. Atmos. Terr. Phys., 54*, 243, 1992.

Chapman, J., and E. T. Pierce, Relations between the character of atmospherics and their place of origin, *Proc. IRE, 45*, 804, 1957.

Deeks, D. G., D-region electron distributions in middle latitudes deduced from the reflection of long radio waves, *Proc. R. Soc. London, Ser. A, 291*, 413, 1966.

Dennis, A. S., and E. T. Pierce, The return stroke of the lightning flash to Earth as a source of VLF atmospherics, *Radio Sci., 68D*, 777, 1964.

Fraser-Smith, A. C., and R. A. Helliwell, The Stanford University ELF/VLF radiometer project: Measurement of the global distribution of ELF/-VLF electromagnetic noise, *Proc. 1985 IEEE Internat. Symp. Electromagn. Compat.*, 305, 1985.

Hargreaves, J. K., *The Solar-Terrestrial Environment*, Cambridge Univ. Press, New York, 1992.

Hayakawa, M., K. Ohta, and K. Baba, Wave characteristics of tweek atmospherics deduced from the direction-finding measurement and theoretical interpretation, *J. Geophys. Res., 99*, 10733, 1994.

Jean, A. G., W. L. Taylor, and J. R. Wait, VLF phase characteristics deduced from atmospheric wave forms, *J. Geophys. Res., 65*, 907, 1960.

Jones, D. L., Electromagnetic radiation from multiple return strokes of lightning, *J. Atmos. Terr. Phys., 32*, 1077, 1970.

Kim, H., and H. Ling, Wavelet analysis of radar echo from finite-size targets, *IEEE Trans. Antennas Propag., 41*, 200, 1993.

Kumar, S., S. K. Dixit, and A. K. Gwal, Propagation of tweek atmospherics in the Earth-ionosphere waveguide, *Nuovo Cimento, 17C*, 275, 1994.

Lanzerotti, L. J., D. J. Thomson, C. G. Maclennan, K. Rinnert, E. P. Krider, and M. A. Uman, Power spectra at radio frequency of lightning return stroke waveforms, *J. Geophys. Res., 94*, p. 13221, 1989.

Mathews, J. D., J. K. Breakall, and S. Ganguly, The measurement of diurnal variations of electron concentration in the 60–100 km ionosphere at Arecibo, *J. Atmos. Terr. Phys., 44*, 441, 1982.

Mechtly, E. A., S. A. Bowhill, L. G. Smith, and H. W. Knoebel, Lower ionosphere electron concentration and collision frequency from rocket measurements of Faraday rotation, differential absorption, and probe current, *J. Geophys. Res., 72*, 5239, 1967.

Morfitt, D. G., and C. H. Shellman, MODESRCH: An improved computer program for obtaining ELF/VLF/LF mode constants in an Earth-ionosphere waveguide, *Interim Rep. 77T*, Nav. Electron. Lab. Cent., San Diego, Calif., 1976.

Narcisi, R. S., Discussion, in *Meteorological and Chemical Factors in D-Region Aeronomy: Record of the Third Aeronomy Conference, Aeron. Rep. 34*, p. 284, Univ. of Illinois, Urbana, 1969. (Re-

produced in *Handbook of Geophysics and the Space Environment*, edited by Adolph S. Jursa, p. 21-55, Air Force Geophys. Lab., Air Force Syst. Command, U.S. Air Force, Springfield, Va, 1985).

Narcisi, R. S., Composition studies of the lower ionosphere, in *Physics of the Upper Atmosphere*, edited by F. Verniani, Ed. Compositori, Bologna, Italy, 1971. (Reproduced in *Handbook of Geophysics and the Space Environment*, edited by Adolph S. Jursa, p. 21-56, Air Force Geophys. Lab., Air Force Syst. Command, U.S. Air Force, Springfield, Va, 1985).

Narcisi, R. S., and A. D. Bailey, Mass spectrometric measurements of positive ions at altitudes from 64–112 kilometers, *J. Geophys. Res., 70*, 3687, 1965.

Pappert, R. A., and J. A. Ferguson, VLF/LF mode conversion model calculations for air to air transmissions in the Earth-ionosphere waveguide, *Radio Sci., 21*, 551, 1986.

Pappert, R. A., and W. F. Moler, Propagation theory and calculations at lower extremely low frequencies (ELF), *IEEE Trans. Commun., 22*, 438, 1974.

Rafalsky, V. A., A. V. Shvets, and M. Hayakawa, One-site distance-finding technique for locating lightning discharges, *J. Atmos. Terr. Phys., 57*, 1255, 1995.

Ryabov, B. S., Tweek propagation peculiarities in the Earth-ionosphere waveguide and low ionosphere parameters, *Adv. Space Res., 12*, (6)255, 1992.

Sechrist, C. F., Jr., Comparisons of techniques for measurement of D-region electron densities, *Radio Sci., 9*, 137, 1974.

Sukhorukov, A. I., ELF-VLF atmospheric waveforms under night-time ionospheric conditions, *Ann. Geophys., 14*, 33, 1996.

Taylor, W. L., VLF attenuation for east-west and west-east daytime propagation using atmospherics, *J. Geophys. Res., 65*, 1933, 1960.

Thomas, L., and M. D. Harrison, The electron density distributions in the *D*-region during the night and pre-sunrise period, *J. Atmos. Terr. Phys., 32*, 1, 1970.

Thomson, N. R., Experimental daytime VLF ionospheric parameters, *J. Atmos. Terr. Phys., 55*, 173, 1993.

Wait, J. R., and K. P. Spies, Characteristics of the Earth-ionosphere waveguide for VLF radio waves, *Tech. Note 300*, Nat. Bur. of Stand., Boulder, Colo., 1964.

Weidman, C. D., and E. P. Krider, The amplitude spectra of lightning radiation fields in the interval from 1 to 20 MHz, *Radio Sci., 21*, 964, 1986.

Yamashita, M., Propagation of tweek atmospherics, *J. Atmos. Terr. Phys., 40*, 151, 1978.

Yedemsky, D. Y., B. S. Ryabov, A. Y. Shehokotov, and V. S. Yarotsky, Experimental investigation of the tweek field structure, *Adv. Space Res., 12*, (6)251, 1992.

T. F. Bell and U. S. Inan, STAR Laboratory, Stanford University, Durand 324, Stanford, CA 94305-9515.

S. A. Cummer, Laboratory for Extraterrestrial Physics, NASA Goddard Space Flight Center, Code 690, Greenbelt, MD 20771. (e-mail: steve.cummer@gsfc.nasa.gov)

(Received May 11, 1998; revised July 10, 1998; accepted July 16, 1998.)